Nuclear Scalar Spin−Spin Couplings and Geometries of Hydrogen Bonds

Hans Benedict,[†] Ilja G. Shenderovich,[†,||] Olga L. Malkina,[‡,§] Vladimir G. Malkin,[§] Gleb S. Denisov,[||] Nikolai S. Golubev,[†,||] and Hans-Heinrich Limbach*[,†]

Contribution from the Institut für Chemie der Freien Universität Berlin, Takustrasse 3, D-14195 Berlin, Germany, Computing Center and Institute of Inorganic Chemistry of the Slovak Academy of Sciences, Bratislava, Slovakia, and Institute of Physics, St. Petersburg State University, 198904 St. Petersburg, Russian Federation

Received March 8, 1999. Revised Manuscript Received December 7, 1999

Abstract: Ab initio calculations of the scalar coupling constants $^1J_{^{15}N-^1H} \equiv J_{NH}$ and $^2J_{^{15}N\cdots^{15}N} \equiv J_{NN}$ of the N−H···N hydrogen bonds in the anion $[C{\equiv}^{15}N\cdots L\cdots{}^{15}N{\equiv}C]^-$ (**1**), L = H, D, and of the cyclic hydrogen-bonded formamidine dimer $(HCNHNH_2)_2$ (**2**) have been performed using the density functional formalism as a function of the hydrogen bond and molecular geometries. The coupling constants are discussed in comparison with the experimental and calculated constants $^1J_{^{19}F-^1H} \equiv J_{FH}$ and $^2J_{^{19}F-^{19}F} \equiv J_{FF}$ reported previously as first set of examples of scalar couplings across hydrogen bonds for the hydrogen-bonded clusters of $[F(HF)_n]^-$, $n = 1-4$ by Shenderovich, I. G.; Smirnov, S. N.; Denisov, G. S.; Gindin, V. A.; Golubev, N. S.; Dunger, A.; Reibke, R.; Kirpekar, S.; Malkina, O. L.; Limbach, H. H. *Ber. Bunsen-Ges. Phys. Chem.* **1998**, *102*, 422. Using the valence bond order model, which has been successfully applied previously to explain hydrogen bond correlations in crystallography and solid-state NMR of hydrogen-bonded systems, the coupling constants are related to the hydrogen bond geometries and NMR chemical shifts. In terms of this model, there is no principal difference between FHF- and NHN hydrogen-bonded systems. Whereas the coupling constant values calculated using the DFT method for the fluorine case only reproduce the experimental trends, the agreement between theory and experiment is much better in the nitrogen cases, which allows one to determine the hydrogen bond geometries including the hydrogen bond angle from a full set of experimental coupling constants. It is found that the coupling constants J_{AB} in A−H···B are proportional to the product of valence bond orders $(p_{AH}p_{HB})^m$, where m is an empirical parameter equal to 2 in the case of fluorine bridge atoms and close to 1 in the case of nitrogen bridge atoms. The coupling constants J_{AH} depend on two terms, a positive term proportional to p_{AH} and a negative term proportional to $p_{AH}(p_{HB})^2$ leading to vanishing or even negative values of J_{AH} at larger A···H distances; in this region the constants J_{AB} are larger than the absolute values of J_{AH}. As a consequence, vanishing couplings between a hydrogen-bonded proton to a heavy nucleus across the hydrogen bond cannot be taken as an indication for a noncovalent character of this hydrogen bond. The existence of J_{AB} is taken as a strong evidence for the covalent character of the hydrogen bonds studied. This is corroborated by a analysis of the molecular orbitals of (**1**) and their individual contributions to the coupling constants.

Introduction

Hydrogen bonding is an important phenomenon in chemistry and biology. In the past, its origin has mostly been attributed to electrostatic interactions between a proton donor AH and an acceptor B forming the bridge A−H···B.[1] On the other hand, several experimental observations have recently provided evidence for a covalent character of the hydrogen bond.

The first evidence refers to correlations of hydrogen bond geometries[2−6] which have been explained in terms of the valence bond order concept of Pauling.[2] In this concept the chemical bond between A and H in a diatomic molecule AH or between H and B in HB can be characterized by empirical valence bond orders p_{AH} and p_{HB} which decay exponentially with the bond distances r_{AH} and r_{HB}

* Address correspondence to this author. E-mail: limbach@chemie.fu-berlin.de. Presented as a plenary lecture at the 40th Experimental NMR Conference, Orlando, Florida, February 28, 1999.

† Freie Universität Berlin.
‡ Computing Center of the Slovak Academy of Sciences.
§ Institute of Inorganic Chemistry of the Slovak Academy of Sciences.
|| St. Petersburg State University.

(1) (a) *The Hydrogen Bond;* Schuster, P., Zundel, G., Sandorfy, C., Eds.; North-Holland Publ. Co.: Amsterdam, 1976. (b) Jeffrey, G. A.; Saenger, W., *Hydrogen Bonding in Biological Structures*; Springer-Verlag: Berlin, 1991. (c) Ratajczak, H.; Orville-Thomas, W. J., *Molecular Interactions;* John Wiley & Sons: Chichester, New York, Brisbane, Toronto, 1980; Vol 1.

(2) (a) Pauling, L. *J. Am. Chem. Soc.* **1947**, *69*, 542. (b) Brown, I. D. *Acta Crystallogr.* **1992**, *B48*, 553. (c) Dunitz, D. *Philos. Trans. R. Soc. London* **1975**, *B 272*, 99.

(3) (a) Truhlar, D. G. *J. Am. Chem. Soc.* **1972**, *94*, 7854. (b) Agmon, N. *Chem. Phys. Lett.* **1977**, *45*, 343.

(4) (a) Steiner, Th.; Saenger, W. *Acta Crystallogr.* **1994**, *B50*, 348. (b) Steiner, Th., *J. Chem. Soc., Chem. Commun.* **1995**, 1331. (c) Gilli, P.; Bertolasi, V.; Ferretti, V.; Gilli, G. *J. Am. Chem. Soc.* **1994**, *116*, 909. (d) Steiner, Th. *J. Phys. Chem. A* **1998**, *102*, 7041.

(5) (a) Benedict, H.; Hoelger, C.; Aguilar-Parrilla, F.; Fehlhammer, W. P.; Wehlan, M.; Janoschek, R.; Limbach, H. H. *J. Mol. Struct.* **1996**, *378*, 11. (b) Benedict, H.; Limbach, H. H.; Wehlan, M.; Fehlhammer, W. P.; Golubev, N. S.; Janoschek, R. *J. Am. Chem. Soc.* **1998**, *120*, 2939. (c) Ramos, M.; Alkorta, I.; Elguero, J.; Golubev, N. S.; Denisov, G. S.; Benedict, H.; Limbach, H. H. *J. Phys. Chem.* **1997**, *A101*, 9791.

(6) (a) Alkorta, I.; Rozas, I.; Elguero, J. *Struct. Chem.* **1998**, *9*, 243. (b) Bader, R. F. W. *Atoms in Molecules. A Quantum Theory*; Oxford University Press: New York, 1990.

10.1021/ja9907461 CCC: $19.00
Published on Web 02/19/2000

$$p_{AH} = \exp\{-(r_{AH} - r_{AH}^{o})/b_{AH}\}, \quad p_{HB} = \exp\{-(r_{HB} - r_{HB}^{o})/b_{HB}\} \quad (1)$$

r_{AH}^{o} and r_{HB}^{o} are the equilibrium bond distances where the valence bond orders are unity, and b_{AH} and b_{HB} represent the parameters describing the bond order decrease. In the case of a hydrogen-bonded complex A−H···B the same hydrogen is bound both to A and to B, but the total valency of hydrogen remains unity, that is

$$p_{AH} + p_{HB} = 1 \quad (2)$$

Equation 2 implies that there is no qualitative but only a quantitative difference between the usual "covalent" bond AH− exhibiting a larger (but nevertheless smaller than 1) valence bond order—and the hydrogen bond HB exhibiting the smaller valence bond order. Thus, in principle, both bonds can be regarded either as "covalent" bonds or as "hydrogen" bonds. If one uses broken lines in order to indicate partial bonds, one should then symbolize a hydrogen-bonded complex as A···H··· B rather than as A−H···B. A second consequence of eq 2 is that for any stationary state the two bond distances r_{AH} and r_{HB} of a hydrogen bond cannot be varied independently. This correlation has been used in tracing reaction pathways of proton-transfer reaction,[3] but it has been verified by neutron crystallography only recently[4] for a number of hydrogen-bonded systems. Some of us have reproduced this correlation recently by numerical quantum mechanical calculations for the case of the anion $[C{\equiv}{}^{15}N{\cdots}H{\cdots}{}^{15}N{\equiv}C]^-$ (**1**) and by solid-state NMR for the same anion as a ligand between two $Cr(CO)_5$ residues;[5a,b] furthermore, the correlation was found to be fulfilled also in the case of hydrogen-bonded complexes between simple acids and ammonia.[5c] These findings incited some of us to link various other hydrogen bond properties such as geometric H/D isotope effects, zero-point energy changes and chemical shifts to the valence bond orders established crystallographically.[5b] Unfortunately, direct quantum mechanical calculations of valence bond orders corresponding to the empirical values are not easy. Using the atom in molecules technology, Bader has shown that the valence bond orders are related to the electron density in the bond critical points.[6b]

A second type of evidence for the covalent character of the hydrogen bonds was provided recently by Isaacs et al.[7] who measured the Compton profile anisotropies of ordinary ice by X-ray methods. The results were not in agreement with an electrostatic character of the hydrogen bond but only with a covalent character, that is, the presence of molecular orbitals extending across the hydrogen bond. Such extended orbitals imply correlated changes of the phase of the corresponding wave function in both parts of the hydrogen-bonded species.

The topic of this paper concerns the third type of evidence to look in a new way at hydrogen-bonded systems, that is, the recent discovery of scalar nuclear spin−spin coupling across hydrogen bonds. These couplings were previously considered as nonexistent, in agreement with the idea that only nuclei in a stable molecular frame held together by covalent bonds experience this type of interaction. By contrast, hydrogen bonds between small molecules are broken and formed rapidly under usual conditions. Therefore, it was a surprise to recognize that such couplings can be observed provided that the lifetime of the hydrogen bonds is sufficiently long.[8−10] This regime has been achieved for small model systems by low-temperature liquid-state NMR using deuterated gases as NMR solvents,[8,9] or in the case of large biomolecules under normal conditions.[10] An important outcome of these studies was that complexes of the type A−H···B can exhibit scalar two-bond couplings $^2J_{A\cdots B} \equiv J_{AB}$ which are larger than the corresponding one-bond coupling constants $^1J_{AH}$ and $^1J_{HB}$, in contrast to any chemical intuition. Examples were $F-H{\cdots}F^-$ hydrogen bonds in clusters of the type $[F(HF)_n]^-$, $n = 2-3$ dissolved in liquefied Freon mixtures,[8] where $|^2J_{FF}| \gg |^1J_{FH}|$. This phenomenon was shown to arise from a sign change of $^1J_{FH}$ when the F···H distance was increased. This sign change was reproduced by quantum chemical calculations[8] using density functional theory implanted in the deMon-NMR code.[11] Thus, absence of coupling of a proton across the hydrogen bond can no longer be taken as an indication for the absence of common molecular orbitals between A and B. In the meantime, scalar heavy atom hydrogen bond couplings were also observed for a complex of ^{15}N labeled 2,4,6-trimethylpyridine with HF dissolved in deuterated Freons,[9a] where a very large value of $J_{FN} = 95$ Hz contrasted with small values of J_{FH}. This observation indicates that the two-bond couplings do not simply scale with the associated gyromagnetic moments. A series of new scalar couplings across hydrogen bonds were observed in biological macromolecules,[10a] mainly due to the work of Dingley and Grzesiek,[10b] where the slow hydrogen bond exchange regime is more easily realized than in small complexes. Thus, evidence for internucleotide $^2J_{NN}$ couplings in ^{15}N labeled nucleic acid base pairs was provided which were of the order of 7 to 8 Hz. This result was confirmed by Pervushin et al.[10c] who reported in addition couplings between protons and ^{15}N across the hydrogen bonds, similar to the H···N couplings observed for O−H···N hydrogen bonds.[9c]

The goal of this paper is to study how the novel couplings across hydrogen bonds are related with the hydrogen bond geometries. We will show that the valence bond order concept is an efficient tool to construct this link between the world of hydrogen bond geometries and scalar couplings. Thus, the geometric hydrogen bond correlations will show up also as correlations of scalar couplings. For this purpose we have used the deMon-NMR code in order to calculate the one- and two bond couplings J_{HN} and J_{NN} of the previously[5a,b] well-studied anion $[C{\equiv}N{\cdots}H{\cdots}N{\equiv}C]^-$ (**1**) as a function of the hydrogen bond geometry. These results will be discussed in comparison

(7) Isaacs, E. D.; Shukla, A.; Platzman, P. M.; Hamann, D. R.; Barbiellini, B.; Tulk, C. A. *Phys. Rev. Lett.* **1999**, *82*, 600.

(8) Shenderovich, I. G.; Smirnov, S. N.; Denisov, G. S.; Gindin, V. A.; Golubev, N. S.; Dunger, A.; Reibke, R.; Kirpekar, S.; Malkina, O. L.; Limbach, H. H. *Ber. Bunsen-Ges. Phys. Chem.* **1998**, *102*, 422.

(9) (a) Golubev, N. S.; Shenderovich, I. G.; Smirnov, S. N.; Denisov, G. S.; Limbach, H. H. *Chem. Eur. Journal* **1999**, *5*, 492. (b) Smirnov, S. N.; Benedict, H.; Golubev, N. S.; Denisov, G. S.; Kreevoy, M. M.; Schowen, R. L.; Limbach, H. H. *Can J. Chem.* **1999**, *77*, 943. (c) Smirnov, S. N.; Golubev, N. S.; Denisov, G. S.; Benedict, H.; Schah-Mohammedi, P.; Limbach, H. H. *J. Am. Chem. Soc.* **1996**, *118*, 4094. (d) Golubev, N. S.; Smirnov, S. N.; Gindin, V. A.; Denisov, G. S.; Benedict, H.; Limbach, H. H. *J. Am. Chem. Soc*. **1994**, *116*, 12055. (e) Golubev, N. S.; Denisov, G. S.; Smirnov, S. N.; Shchepkin, D. N.; Limbach, H. H. *Z. Phys. Chem.* **1996**, *196*, 73.

(10) (a) Borman, S. *Chem. Eng. News* **1999**, *77*, 36. (b) Dingley, A. J., Grzesiek, S. *J. Am. Chem. Soc.* **1998**, *120*, 8293. (c) Pervushin, K.; Ono, A.; Fernández, C.; Szyperski, T.; Kainosho, M.; Wüthrich, K. *Proc. Natl. Acad. Sci. U.S.A.* **1998**, *95*, 14147.

(11) (a) deMon-NMR program: Salahub, D. R.; Fournier, R.; Mlynarski, P.; Papai, I.; St-Amant, A.; Ushio, J. In *Density Functional Methods in Chemistry*; Labanowski, J., Andzelm, J., Eds.; Springer, New York, 1991; St-Amant, A.; Salahub, D. R.; *Chem. Phys. Lett.* **1990**, *169*, 387. (b) Malkin, V. G.; Malkina, O. L.; Casida, M. E.; Salahub, D. R. *J. Am. Chem. Soc.* **1994**, *116*, 5898. (c) Malkin, V. G.; Malkina, O. L.; Eriksson, L. A.; Salahub, D. R.; *Modern Density Functional Theory: A Tool for Chemistry*; Seminario, J. M., Politzer, P., Eds.; Elsevier: Amsterdam, 1995; Vol.2. (d) Malkin, V. G.; Malkina, O. L.; Salahub, D. R. *Chem. Phys. Lett.* **1994**, *221*, 91. (e) Malkina, O. L.; Salahub, D. R.; Malkin, V. G. *J. Chem. Phys.* **1996**, *105*, 8793.

Scheme 1

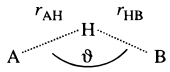

Scheme 2

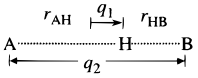

with those obtained for the clusters $[F(HF)_n]^-$, $n = 2-3$ studied previously.[8] In addition we have calculated the coupling constants for the formamidine dimer **2** which is the simplest model for nucleic acid base pairs. The structure and tautomerism of **2** and its derivatives has been studied by liquid- and solid-state NMR[12] and by ab initio calculations.[13] Finally, we will present a detailed analysis of the various molecular orbitals of **1** from which it follows that the common molecular orbitals across the hydrogen bonds are responsible for the associated scalar couplings.

Computational Methods

Ab initio calculations of optimized geometries were performed using the GAUSSIAN 94 program[14] at the MP2/6-31+G(d,p) level. The calculations of the scalar spin−spin coupling constants and chemical shifts were done within the framework of density functional theory (DFT) using the deMon-NMR code.[11] Perdew and Wang exchange[15a] with Perdew correlation[15b] functionals and IGLO-III basis set[15c] were implied.

Data Analysis. As mentioned above, one can associate to any hydrogen-bonded system A−H···B two distances r_{AH} and r_{HB} corresponding to the bond orders p_{AH} and p_{HB}, and an hydrogen bond angle ϑ as indicated in Scheme 1. In the following, we will find it convenient to define additionally the coordinates q_1 and q_2 according to

$$q_1 = {}^1/_2(r_{AH} - r_{HB}), \quad q_2 = r_{AH} + r_{HB} \tag{3}$$

In the case of a linear hydrogen bond q_1 corresponds directly to the distance of the proton with respect to the hydrogen bond center and q_2 to the heavy atom A···B distance, as indicated in Scheme 2.

By combining eqs 1−3, the following relation can been derived[5] for the symmetric case where the heavy acceptor atoms in A and B are identical, that is, $r_{AH}^o = r_{HB}^o = ro$ and $b_{AH} = b_{HB} = b$, from which it follows that

$$q_2 = r_{AH} + r_{HB} = 2\,r^o + 2\,q_1 + 2b\,\ln[1 + \exp\{-2q_1/b\}] \tag{4}$$

In Figure 1a we have plotted q_2 as a function of q_1 in arbitrary units. When the proton is near A, q_1 is negative and q_2 large. In this region the bond order p_{AH} is close to 1 and p_{HB} close to 0 as indicated in

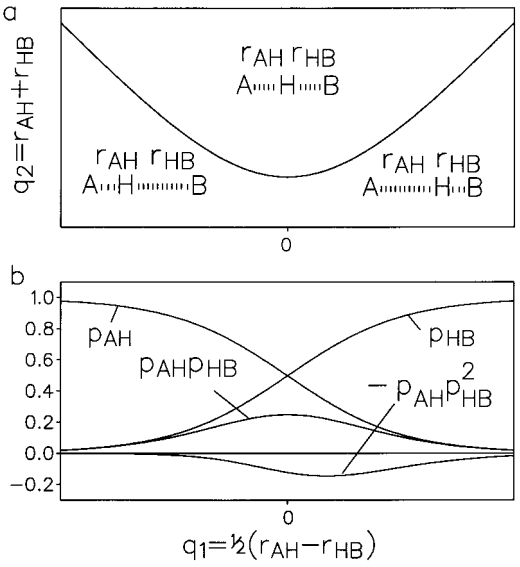

Figure 1. (a) Correlation between the sum $q_2 = r_{AH} + r_{HB}$ of a hydrogen-bonded system A−H···B defined in Scheme 2 and the deviation $q_1 = {}^1/_2(r_1 - r_2)$ of the proton from the hydrogen bond center according to eq 4. (b) Bond order terms as a function of q_1. For further description see text.

Figure 1b. When the proton is shifted toward the hydrogen bond center the A···B distance decreases. q_2 exhibits a minimum at $q_1 = 0$. At this point the two bond orders $p_{AH} = p_{HB} = {}^1/_2$. When the proton is shifted toward B the A···B distance increases again. We note that the product $p_{AH}p_{HB}$ is zero in the two limiting cases but exhibits a maximum at $q_1 = 0$, as indicated in Figure 1b. We have included also the term $-p_{AH}p_{HB}^2$ in Figure 1b which we will need below.

In ref 5b it was shown that various hydrogen bond properties can be expanded in terms of derivatives of the correlation $q_2 = f(q_1)$. Recently,[9b] some of us showed that certain quantities are conveniently expressed directly as a function of the valence bond orders. For example, the ^{15}N chemical shift of a base B such as pyridine in A−H···B− where A = RO and B = pyridine−was found to be related to the valence bond order p_{HB} by

$$\delta_B = \delta_B^{\infty} - (\delta_B^{\infty} - \delta_{HB}^{o})p_{HB} \tag{5}$$

where the parameters δ_B^{∞} and δ_{HB}^{o} are the values for the free base and for the free donor HB characterized by r_{HB}^o. For the ^1H chemical shifts of the hydrogen bond proton the equation

$$\delta(^1H) = \Delta_H(4p_{AH}p_{HB})^m + \delta_{AH}^{o}\,p_{AH} + \delta_{HB}^{o}\,p_{HB} \tag{6}$$

was reported,[9b] where the data could well be adapted by setting $m = 1$. In the following, we will take m as an adaptable parameter. Δ_H is the excess chemical shift of the quasisymmetric complex and δ_{AH}^o and δ_{HB}^o are the limiting chemical shifts corresponding to the distances r_{AH}^o and r_{HB}^o. As mentioned previously,[5b,9b] it is clear that the above equations imply a correlation between $\delta(^1H)$ and $\delta(^{15}N)$, which is the manifestation in the world of NMR parameters of the geometric correlations r_{AH} with r_{HB} (or q_1 with q_2). The $^{15}N-^1H$ chemical shift correlation was verified also experimentally for the case of complexes of pyridine with various acids dissolved in Freons.[9]

In the following we apply the valence bond concept to the problem of scalar couplings in hydrogen-bonded systems. In diatomic molecules such as HD, Hush et al.[16] has shown theoretically that the scalar nuclear coupling is directly proportional to the bond order. If more than two atoms are involved the situation is more complicated. For example, when the HD-molecule is inserted into a transition metal complex L_nM

(12) (a) Meschede, L.; Gerritzen, D.; Limbach, H. H. *Ber. Bunsen-Ges. Phys. Chem.* **1988**, *92*, 5669. (b) Limbach, H. H.; Meschede, L.; Scherer, G. *Z. Naturforsch.* **1989**, *44a*, 459. (c) Meschede L.; Limbach, H. H. *J. Phys. Chem.* **1991**, *95*, 10267. (d) Männle F.; Wawer, I.; Limbach, H. H. *Chem. Phys. Lett.* **1996**, *256*, 657. (e) Anulewicz, R.; Wawer, I.; Krygowski, T. M.; Männle, F.; Limbach, H. H. *J. Am. Chem. Soc.* **1997**, *119*, 12223.

(13) (a) Svensson, P.; Bergmann, N. A.; Ahlberg, P. *Z. Naturforsch.* **1989**, *44a*, 473. (b) Nguyen, K. A.; Gordon, M. S.; Truhlar, D. G. *J. Am Chem, Soc.* **1991**, *113*, 1596.

(14) Frisch, M. J.; Trucks, G. W.; Schlegel, H. B.; Gill, P. M. W.; Johnson, B. G.; Robb, M. A.; Cheeseman, J. R.; Keith, T.; Petersson, G. A.; Montgomery, J. A.; Raghavachari, K.; Al-Laham, M. A.; Zakrzewski, V. G.; Ortiz, J. V.; Foresman, J. B.; Cioslowski, J.; Stefanov, B. B.; Nanayakkara, A.; Challacombe, M.; Peng, C. Y.; Ayala, P. Y.; Chen, W.; Wong, M. W.; Andres, J. L.; Replogle, E. S.; Gomperts, R.; Martin, R. L.; Fox, D. J.; Binkley, J. S.; Defrees, D. J.; Baker, J.; Stewart, J. P.; Head-Gordon, M.; Gonzalez, C.; Pople, J. A. *Gaussian 94*, revision D.3; Gaussian, Inc.: Pittsburgh, PA, 1995.

(15) (a) Perdew, J. P.; Wang, Y. *Phys. Rev.* **1986**, *B* 33, 8800. (b) Perdew, J. P. *Phys. Rev.* **1988**, *A 38*, 3098. (c) Kutzelnigg, W.; Fleischer, U.; Schindler, M. *NMR-Basic Principles and Progress*; Springer, Heidelberg, **1990**, *23*, 165.

(16) (a) Craw, J. S.; Bacskay, G. B.; Hush, N. S. *J. Am. Chem. Soc.* **1994**, *116*, 5937. (b) Bacskay, G. B.; Bytheway, I.; Hush, N. S. *J. Am. Chem. Soc.* **1996**, *118*, 3753. (c) Hush, N. S. *J. Am. Chem. Soc.* **1997**, *119*, 1717.

giving a dihydride L_nMHD, the positive one-bond coupling between H and D becomes gradually a negative two-bond coupling.[17]

Here, we assume that the heavy atom coupling J_{AB} through a hydrogen bridge A−H···B is proportional to the m^{th} power of the bond order product

$$J_{AB} = J_{AB}^{o}(\vartheta)(4p_{AH}\,p_{HB})^{m},$$
$$J_{AB}^{o}(\vartheta) = J_{AB}^{o}(180)[1 + c(\vartheta - 180)^2] \quad (7)$$

$J_{AB}^{o}(\vartheta)$ corresponds to the value of the coupling at $p_{AH} = p_{HB} = 0.5$, that is, in the symmetric case to the maximum coupling. Later we will show that $J_{AB}^{o}(\vartheta)$ depends on the hydrogen bond angle ϑ, where we assume a quadratic dependence described by a parameter c; m is the same empirical parameter as in eq 6.

We express the coupling constant J_{AH} as the sum of a term linear to the valence bond order p_{AH} and the nonlinear second-order term depicted in Figure 1b, that is The parameters in eq 8 do not seem to depend on

$$J_{AH} = J_{AH}^{o}p_{AH} + 8\Delta J_{AH}p_{AH}p_{HB}^{2} \quad (8)$$

the hydrogen bond angle ϑ. The parameter ΔJ_{AH} represents the deviation of J_{AH} from $J_{AH}^{o}/2$ at the symmetric point where $p_{AH} = p_{HB} = {}^1/_2$. It will be shown later that ΔJ_{AH} is negative. The consequence of the negative sign will be that at certain distances the two terms in eq 8 cancel each other leading to $J_{AH} = 0$, whereas the coupling constant J_{AB} will remain nonzero.

To determine the parameters of the above equations from the experimental and calculated data we wrote an appropriate computer program. In a first stage of the calculations an arbitrary set of q_1 values was defined from which we calculated q_2, then r_{AH} and r_{HB} and the corresponding bond orders p_{AH} and r_{HB} using the values of r_{AH}^{o} and b_{AH}^{o} determined previously.[5,8] The parameters m, J_{AB}^{o}, J_{AH}^{o}, ΔJ_{AH}, Δ_H, $\delta_{AH}^{o} = \delta_{HB}^{o}$ were then obtained by eye-fitting of the functions of interest to the corresponding data sets.

Results and Discussion

^{19}F−H···^{19}F Hydrogen-Bonded Systems. In ref 8 some of us had reported the low-temperature NMR spectra of hydrogen-bonded clusters $[F(HF)_n]^-$, $n = 1-4$ using N-tetrabutylammonium as counterion and CDF_3/CDF_2Cl as solvent. As the slow hydrogen bond exchange regime could be reached the individual complexes with $n = 1-3$ could be characterized by their ^{1}H and ^{19}F chemical shifts and couplings constants; the complex with $n = 4$ was partially characterized. The relative sign of the coupling constants was obtained by interpretation of the differential widths of various multiplet lines. Ab initio calculations at the MP2/6-31+G(p,d) level were carried out leading to the calculated structures with the following symmetries of $[F(HF)_n]^-$, $n = 1-4$ as $D_{\infty h}$, C_{2v}, D_{3h}, and T_d, in agreement with the average solution symmetries obtained by NMR. Within the margin of error, the hydrogen bonds were linear. In addition, chemical shifts and coupling constants of these complexes were calculated using the deMon-NMR code.

The hydrogen bond geometries of the complexes can be characterized by the graph of Figure 2a where we have plotted the F···F distances, that is, $q_2 = r_{FH} + r_{HF}$ as a function of the deviation $q_1 = {}^1/_2(r_{FH} - r_{HF})$ of the proton from the hydrogen bond center. We define this deviation to be positive for the central fluorine and negative for the terminal fluorine nuclei. Therefore, the complexes $[F(HF)_n]^-$ provide a kind of reaction pathway for the transfer of the proton from one fluorine to the other.

The solid line represents the correlation curve eq 4, using the parameters of Table 1. When the proton is on the left fluorine

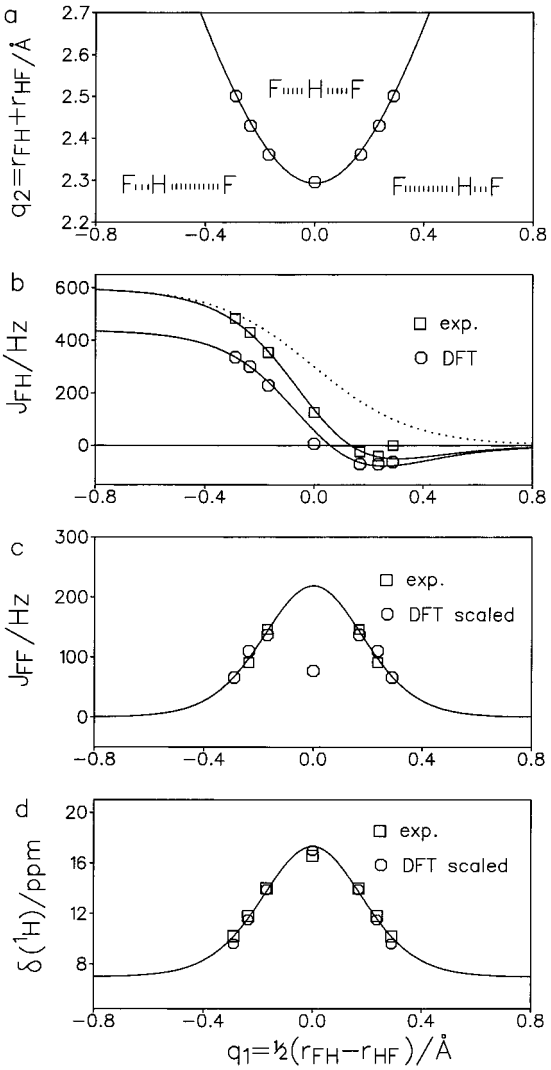

Figure 2. Experimental and calculated properties of fluoride−HF complexes as a function of the deviation $q_1 = {}^1/_2(r_{FH} - r_{HF})$ of the proton from the hydrogen bond center. q_1 is positive for the central and negative for the terminal fluorine nuclei and obtained using ab initio calculations at the MP2/6-31+G(d,p) level (Table 1). (a) Calculated F···F distances $q_2 = r_{FH} + r_{HF}$. (b) Experimental and calculated coupling constants J_{FH} and (c) J_{FF}. (d) Experimental and calculated ^{1}H NMR chemical shifts. The data are taken from ref 8. The solid lines are calculated according to the valence bond model as described in the text.

the F···F distance is large but decreases when the proton is shifted into the hydrogen bond center and increases again when the proton is shifted across the center. The shortest distance of about 2.3 Å is reached in the symmetric bifluoride anion where the F···H distances are 1.15 Å.

Figure 2, b and c, shows graphs of the coupling constants J_{FH} and J_{FF} as a function of q_1. If we refer to a given fluorine atom, its coupling with the hydrogen bond proton J_{FH} is large when the distance is small; the coupling J_{FF} across the hydrogen bond is small. When the F···H distance is increased, J_{FH} decreases because of the decrease of the F···H bond order corresponding to the first term in eq 8 as depicted by the dotted curve in Figure 2b; however, J_{FF} increases, exhibits a maximum at the shortest F···F distance at $q_1 = 0$ and decreases again. At larger distances the negative second-order term in eq 8 becomes so large that J_{FH} goes through zero and becomes negative; eventually at very large F···H distances all couplings again approach zero. It is very important to note that in the region of

(17) Gründemann, S.; Limbach, H. H.; Buntkowsky, G.; Sabo-Etienne, S.; Chaudret, B. *J. Phys. Chem. A.* **1999**, *103*, 4752.

Table 1. Parameters of Hydrogen Bond Correlation and Scalar Coupling Constants in FHF^- and NHN^- Hydrogen Bonds

compound	A, B	R_{AH}^o (Å)	ϑ (deg)	b_{AH} (Å)	m	c	δ_{AH}^o	ΔH	J_{AH}^o	ΔJ_{AH}	J_{AB}^o (180)
$[F(HF)_n]^-$	^{19}F	0.897	180	0.36[a]	2	-	7	10.3	600	−162.5	220
1	^{15}N	0.99[b]	180−150	0.404[b]	1	0.001	−4	16.25	123	−17.5	24.3
2	^{15}N	0.99[b]	175.4	0.404[b]	1	0.001	-	-	93	−17.5	24.3

[a] Determined from Figure 2a. [b] From ref 5b. For the definition of the parameters see eqs 1−8. Coupling constants in Hz, chemical shifts δ in ppm.

the sign change of J_{FH}, the heavy atom coupling J_{FF} is much larger than J_{FH}. Without the negative term the result would be different as indicated by the dotted line in Figure 2b.

The absence of scalar coupling of the proton across the hydrogen bond is, therefore, not caused by a purely electrostatic character of the hydrogen bond which manifests its covalent character in the large J_{FF} values. We note that the values are of the order of the geminal FCF couplings in saturated fluorocarbons (160−290 Hz), and even larger than the value of 95 Hz found for the fluorine-bridged anion, $[F_3B-F-BF_3]^-$.[18]

In Figure 2, b and c, we have also included values calculated using the deMon-NMR code (in Figure 2c, a shift of 210 Hz was added to each calculated value for better comparison with experiment). Overall, the calculated values follow the experimental trend, especially the sign change of J_{FH} at $q_1 = 0.133$ Å which corresponds to $q_2 = 2.344$ Å and hence a F···H distance of 1.305 Å. We note that the calculated values of J_{FH} are systematically smaller than the experimental values, where the offset is about 100 Hz at short F···H distances. As it was pointed out in previous publications [11d] this offset becomes smaller as the distances are increased. The calculations confirm the existence of large values of J_{FF}, but they are about 210 Hz away from the experimental values. Moreover, the value for the symmetric anion is smaller than expected by extrapolation. This type of coupling apparently constitutes the most difficult problem for calculation by the DFT method. We note that the CAS method (complete active space multiconfiguration method) reproduced well the experimental value of $J_{FH} = 124$ Hz with 133 Hz for the bifluoride anion, but the calculated value of $J_{FF} = 385$ Hz value seems to be too large.[8] Therefore, further theoretical studies are necessary to reproduce by theory the experimental data. Note that the anharmonicity of the potential of the proton motion and hence vibrational averaging might also play a role which were not taken into account here.

In Figure 3a the coupling constants J_{FH} and J_{FF} are depicted as a function of the other hydrogen−fluorine coupling constants J_{HF}. This graph exhibits a very characteristic pattern and is useful as it does not rely on additional experimental or calculated values of the hydrogen bond geometry. Figure 3b shows that there is an almost linear relation between J_{FF} and the proton chemical shifts $\delta(^1H)$.

Let us now discuss the solid lines in Figures 2, b and c, and 3 which were calculated using eqs 7 and 8, the parameters of the correlation curve of Figure 1a, and the constants listed in Table 1. The agreement between the solid lines and the experimental data points is very satisfactory, using a value of $m = 2$ in eqs 6 and 7, although the body of data is not yet large enough to really confirm the validity of these equations from a quantitative standpoint. At present, these equations also cannot yet be confirmed by the deMon-NMR calculations. Nevertheless, from the solid lines in Figures 2c and 3 we estimate by extrapolation J_{FF} of the bifluoride ion to be about 220 Hz.

The C≡N···H···N≡C$^-$ Anion. To know whether the results obtained experimentally and theoretically for the FHF-hydrogen bonds are also reliable for NHN-hydrogen bonds we performed deMon-NMR calculations on the C≡N···H···N≡C$^-$ anion. The equilibrium geometries and various hydrogen bond properties were already calculated previously[5] as a function of the distance to a Li^+ cation. The hydrogen bond was found to be linear, and the data were compared to those obtained experimentally by solid-state NMR for the anion as ligand between two $Cr(CO)_5$ moieties.[5] In the case of large C···Li^+ distances the proton was found to move in a low-barrier hydrogen bond where the barrier was smaller than the zero-point energies of the proton and the deuteron. At shorter C···Li^+ distances the proton moved away to the nitrogen which was more distant to the Li^+ ion. In these cases the proton motion took place in asymmetric single-well potentials exhibiting well-characterized geometries. H/D-isotope effects and zero-point energies were calculated and correlated with the hydrogen bond geometries.[5b] A very important result was that a hydrogen bond correlation between q_1 and q_2 of the type of eq 4 was realized as represented by the solid line in Figure 4a and the parameters $b = 0.404$ Å and $r_{NH}^o = 0.99$ Å published previously.[5b] Again, this correlation indicates that the NN distance contracts when the proton is shifted toward the hydrogen bond center, where the shortest NN-distance is 2.54 Å realized in the symmetric complex at $q_1 = 0$. Thus, in the further calculations carried out in this study we could restrict

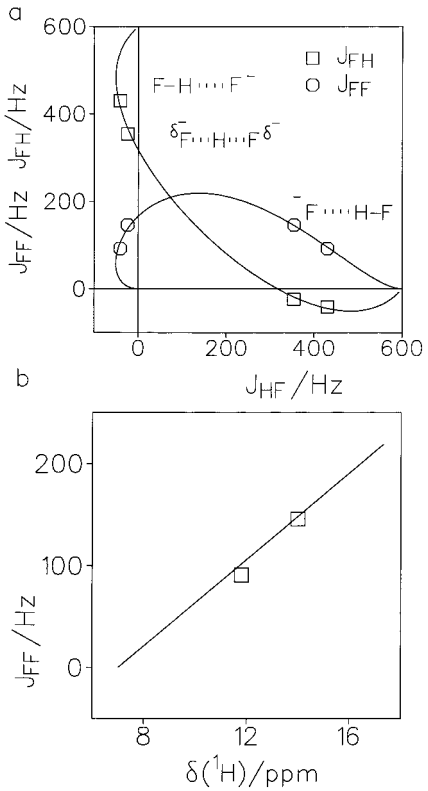

Figure 3. (a) Plot of the experimental coupling constants J_{FH} and J_{FF} as a function of J_{HF}. (b) J_{FF} as a function of $\delta(^1H)$. The data are taken from ref 8. The solid lines are calculated according to the valence bond model as described in the text.

(18) Hartman, J. S.; Stilbs, P. *J. Chem. Soc., Chem. Commun.* **1975**, 566.

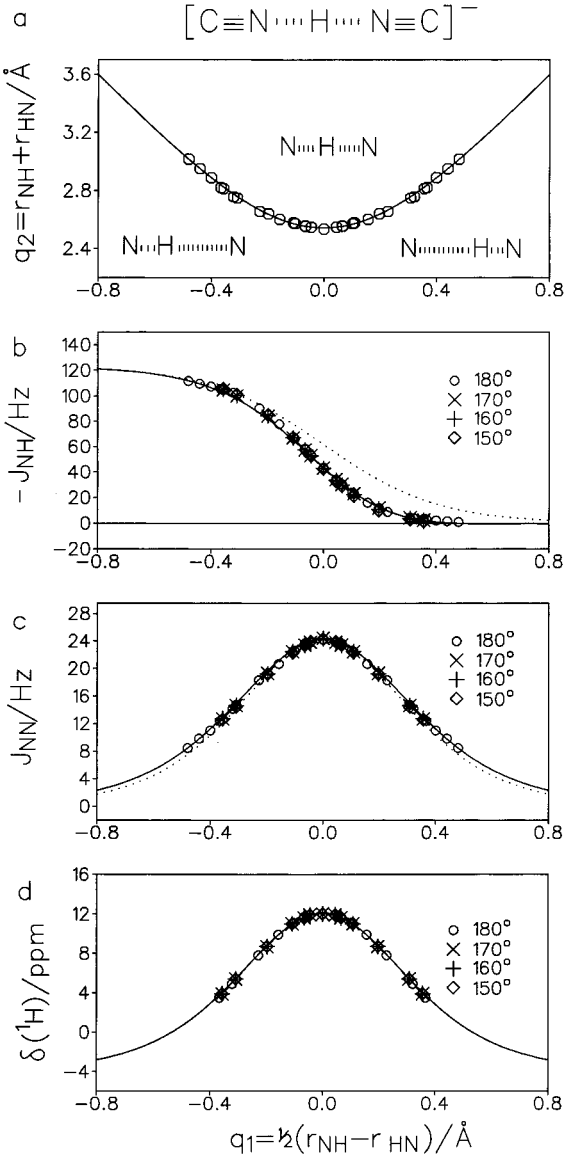

Figure 4. Calculated properties of $[C{\equiv}^{15}N{\cdots}H{\cdots}{}^{15}N{\equiv}C]^-$ (**1**) as a function of q_1. The calculated lines were fitted to the data points using the equations as described in the text. (a) Calculated values q_2 of **1** near Li^+ according to ref 5. (b) Calculated single bond couplings $-J_{NH}$. (c) Calculated two bond couplings J_{NN}. The solid line was calculated according to eq 7 using $m = 0.9$ and the dotted line using $m = 1$. (d) Calculated ^1H chemical shifts according to ref 5.

ourselves to geometries which fulfilled the correlation, which simplified the calculations substantially. However, we additionally changed the hydrogen bond angle ϑ from 180° to 150°, assuming again the validity of the correlation of eq 4.

The results of all present calculations are depicted in Figures 4−6. The solid lines were calculated according to eqs1−8 and the parameters included in Table 1. The values of J_{NH} and J_{NN} are displayed in Figure 4, b and c, as a function of q_1. Qualitatively, we observe a similar behavior of all coupling constants as already discussed for the FHF^- case. The J_{NN} values increase from small zero to a maximum of 24.2 Hz at $q_1 = 0$ and then decrease again. When the N···H distance is increased and the N···H bond order decreased, J_{NH} values also decrease. At larger distances the two-bond term in eq 8 becomes slightly larger than the one-bond term leading to slightly negative values of J_{NH}; again, the absence of the negative term leads to the dotted line in Figure 4b. However, experimentally one would probably only see a vanishing coupling constant.

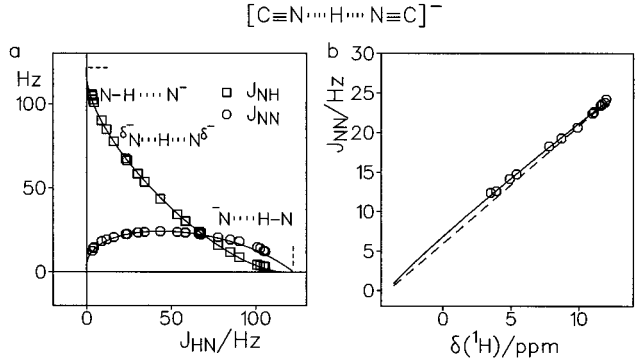

Figure 5. Calculated properties of $[C{\equiv}^{15}N{\cdots}H{\cdots}{}^{15}N{\equiv}C]^-$ (**1**). The calculated lines were fitted to the data points using the equations as described in the text. (a) Calculated coupling constants J_{NH} and J_{NN} as a function of J_{HN}. (b) J_{NN} as a function of $\delta(^1H)$. The calculated chemical shift data points are taken from ref 5.

The calculated values are very well reproduced by eqs 7 and 8, indicating the validity of these equations. Within the margin of error, the coupling constants J_{NH} do not depend on the hydrogen bond angle ϑ, in contrast to the values of J_{NN}. In Figure 4c, for the sake of clarity, we multiplied all calculated values of J_{NN} by the factor $[1 + c(\vartheta - 180)^2]^{-1}$ in eq 7, by setting the parameter $c = 0.001$. As a result, all coupling constants J_{NN} are now placed on the theoretical curve calculated according to eq 7 for $\vartheta = 180°$. We find that setting the parameter $m = 1$ reproduces the data in a satisfactory way (dashed line) although $m = 0.9$ fits the data much better (solid line). As a result, when both J_{NH} and J_{NN} can be measured, it is possible to obtain the hydrogen bond geometry, including the hydrogen bond angle, assuming the validity of the hydrogen bond correlation eq 7.

The value of $J_{NH}{}^o = 123$ Hz obtained by the data fitting is in very good agreement with value of 135 Hz found for $H{-}C{\equiv}{}^{15}N{-}H^+$.[19] Therefore, the deMon-NMR code works much better for couplings with nitrogen than with fluorine as it has been expected.[11c−e] We have to note possible problems in calculation of the dependence of the spin−spin coupling on the gradually increased bond length. For some distances close to the bond-breaking area the HOMO−EnDashLUMO gap might become very small, and the perturbation theory used in the calculations would not work any more. However, such artifacts can easily be detected and excluded.

We have included the dependence of the ^1H chemical shifts $\delta(^1H)$ of the hydrogen bond proton in Figure 4d. The solid line was calculated using eq 6 by adapting the parameters $\Delta_H = 16.25$ ppm and $\delta_{AH}{}^o = \delta_{HB}{}^o = -4$ ppm. The agreement between the values from the valence bond model and the theoretical values is excellent. Thus, both the values J_{NN} and the $\delta(^1H)$ depend on the same valence order product depicted in Figure 1b, as proposed in eqs 6 and 7. As a result it follows as in the fluorine case that there should be a linear relation between the two quantities. This is indeed the case as depicted in Figure 5b, where the solid line was calculated from the parameters determined in Figure 4.

Finally, we have plotted J_{NH} and J_{NN} as a function of J_{HN} in Figure 5a. The calculated lines in Figure 5a reproduce the data in an excellent way. We note that in the case of a series of systems characterized by different equilibrium constants between two limiting tautomeric forms a plot of J_{NH} as a function of

(19) Martin, G.; Martin, M. L.; Gouesnard, J. P. *NMR Basic Principles and Progress*; Springer: Heidelberg, Germany, 1989; Vol. 18, *^{15}N NMR Spectroscopy*.

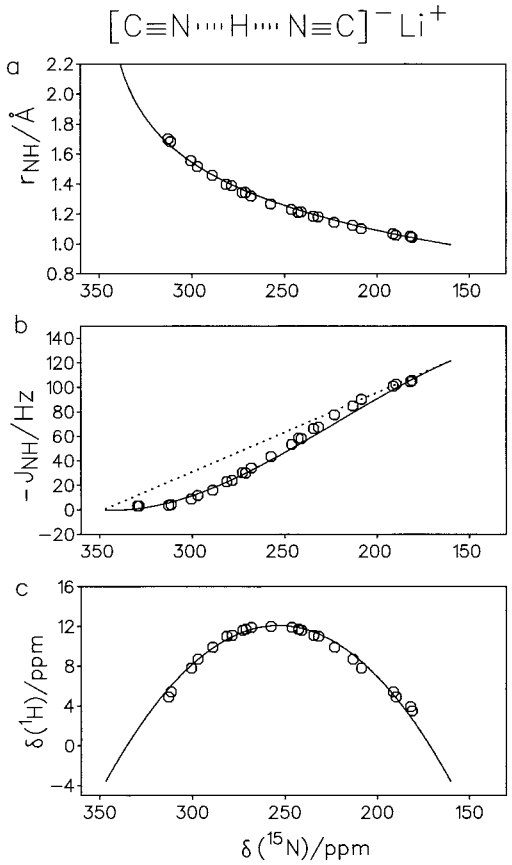

Figure 6. Calculated properties of $[C{\equiv}^{15}N{\cdots}H{\cdots}{}^{15}N{\equiv}C]^-$ (**1**). Calculated (a) distances r_{NH}, (b) $-J_{NH}$ and (c) $\delta(^1H)$ as a function of $\delta(^{15}N)$. The solid lines were calculated using the valence bond model as described in the text. The calculated chemical shift data points are taken from ref 5.

J_{HN} should lead to a straight line with a slope of -1 as proposed in ref 9a. Thus, a graph of the kind shown in Figure 5 will be an important criterion in the future in order to determine whether a system of interest can be described better in terms of an equilibrium between two tautomeric forms or in terms of a series of low-barrier hydrogen bonds.

In Figure 6a we have depicted some interesting properties as a function of the ^{15}N chemical shifts $\delta(^{15}N)$ calculated previously[5b] using the Hartree−Fock IGLO code[15c] for **1**. Figure 6a depicts a plot of the distance r_{NH} as a function of $\delta(^{15}N)$. Here, we use eq 5 in order to accommodate the data, which represents a considerable simplification as compared to the equations reported in ref 5. By eye-fitting we obtain the parameters $\delta_N{}^\infty = 348$ ppm, $\delta_{HN}{}^o = 158$ ppm with reference to solid ammonium chloride. Figure 6b shows how the coupling constant J_{NH} depends on $\delta(^{15}N)$, and we have included again as a dotted line the results without the second term in eq 8. In Figure 6c we plot $\delta(^1H)$ as a function of $\delta(^{15}N)$. The calculated curves using the parameters of Figure 4 reproduce the data in an excellent way.

The Cyclic Formamidine Dimer: A Model for Nucleic Acid Base Pairs. Finally, we have calculated the scalar coupling constants for the cyclic formamidine dimer **2** which is the simplest analogue of nucleic acid base pairs. In these dimers double proton transfers take place which have been studied experimentally[12] and theoretically.[13] The results of all present calculations are assembled in Table 2 and depicted in Figures 7 and 8. The solid lines were calculated according to eqs 1−8 and the parameters included in Table 1. We have considered the ground-state C_2 and the symmetric D_{2h} structure corresponding to a hill-top as calculated by Truhlar et al.[13b] The geometries of Figure 7a reproduce very well the results of Truhlar. As indicated in Figure 7b, for the ground state, the calculated one-bond coupling constant J_{NH} of the NH group exhibiting the short distance is -84 Hz which is in excellent agreement with the values between -85 and 90 Hz reported for formamidines,[12] nucleic acid base pairs[10] and related NH groups exhibiting an sp^2 character. The intramolecular constant J_{NN} is of the order of 5.5 Hz and smaller than the corresponding coupling constant across the hydrogen bond. This value reproduces well the values of about 7 Hz found for experimentally for nucleic acid base pairs.[10b] Moreover, this value is larger than the one-bond coupling $|J_{H\cdots N}|$ across the hydrogen bond as found in the F−H···F case. This latter constant is found to be positive—that is, of opposite sign as compared to the large constant—which is not surprising in view of the fluorine case. As discussed above, the small value is connected with the second-order term in eq 8.

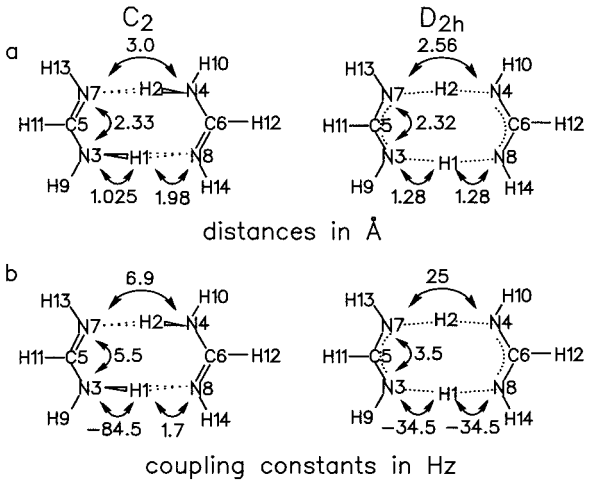

Figure 7. Calculated properties of the cyclic formamidine dimers **2**. Included are the geometries calculated by Truhlar et al.[13b] of the ground state (C_2) and of the symmetric structure D_{2h} corresponding to a hill-top. (a) Calculated distances and (b) calculated coupling constants.

From Figure 8a we note that both configurations fulfill well the universal NHN-hydrogen bond correlation curve taken from ref 5. For the ground state we could expect this result, but not necessarily for the hill-top D_{2h} or other nonstationary states. In Figure 8, b and c, we have assembled the coupling constants J_{NH} and J_{NN} as a function of q_1. The calculated solid line in Figure 8b was calculated using eq 8 by adapting $J_{NH}{}^o$ to 93 Hz as expected for sp^2 nitrogen atoms. The parameter ΔJ_{NH} which is crucial for the H···N coupling across the hydrogen bond was kept constant. $J_{AB}{}^o(174.4°) = 24.3[1 + 0.001(\vartheta - 180)^2] = 25.1$ Hz.

As in the case of **1**, the coupling constants J_{NN} are well reproduced by eq 7 by introducing the hydrogen bond angle of $\vartheta = 174.4°$, $c = 0.001$, and the value of $J_{AB}{}^o(180°) = 24.2$ Hz found for **1**, leading to a maximum value of $J_{AB}{}^o(174.4°) = 25.1$ Hz for the configuration with the shortest NN-distance. Thus, the value of $J_{AB}{}^o(180°)$ seems to be general, independent of the nature of the bridge. We remind that the shortest NN-distance of 2.54 Å was found also to be independent of the nature of the NHN-bond.[5b] These results might be useful in elucidating the structures of nucleic acid base pairs from coupling constants.

Molecular Orbital Analysis and Coupling Constants of the $[C{\equiv}N{\cdots}H{\cdots}N{\equiv}C]^-$ Anion. In this section we will come back to the $[C{\equiv}N{\cdots}H{\cdots}N{\equiv}C]^-$ **1** where we would like to

Table 2. Calculated Geometries and Scalar Coupling Constants in the Cyclic Formamidine Dimer (**2**)

	r(N3,H1) (Å)	*r*(N8,H1) (Å)	*r*(N3,N8) (Å)	*r*(N3,N7) (Å)	ϑ(N3,H1,N8) (deg)	*J*(N3,H1) (Hz)	*J*(N8,H1 (Hz)	*J*(N3,N8) (Hz)	*J*(N3,N7) (Hz)
C_2	1.025	1.978	3.000	2.329	174.2	−84.5	1.7	6.9	5.5
D_2h	1.281	1.281	2.560	2.322	174.5	−34.5	−34.5	25.0	3.5

Additional Data

C_2	*r*(N3,C5) = 1.356 Å, *r*(C5,N7) = 1.297 Å, *r*(N3,H9) = 1.006 Å *r*(C5,H11) = 1.092 Å, *r*(N7,H13) = 1.017 Å ϑ(H1,N3,C5) = 119.1°, ϑ(N3,C5,N7) = 122.7°, ϑ(H9,N3,C5) = 117.7° ϑ(H11,C5,N7) = 123.1°, ϑ(H13,N7,C5) = 109.7°, ϑ(H2,N7,C5) = 120.7° ω(H1,N3,C5,N7) = −13.9°, ω (H9,N3,C5,N7) = −166.2°, ω(H11,C5,N7,N3) = 177.0° ω(H13,N7,C5,N3) = −177.5°, ω(H2,N7,C5,N3) = 13.4°, ω(C5,N7,H2,N4) = −33.2°
D_{2h}	*r*(N3,C5) = 1.323 Å, *r*(N3,H9) = 1.011 Å, *r*(C5,H11) = 1.093 Å ϑ(H1,N3,C5) = 121.4°, ϑ(N3,C5,N7) = 122.7°, ϑ(H9,N3,C5) = 114.2°, ϑ(H11,C5,N7) = 118.6°

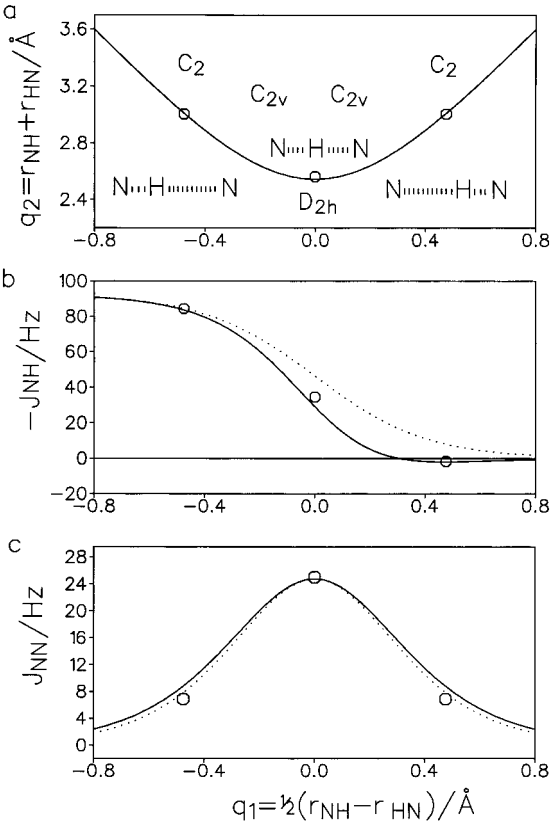

Figure 8. (a) Calculated values q_2 of the cyclic formamidine dimers **2** as a function of q_1. (b) Calculated single bond couplings $-J_{NH}$. (c) Calculated two bond couplings J_{NN}. The calculated lines were fitted to the data points using the equations as described in the text. The solid line was calculated according to eq 7 using $m = 0.9$, $\vartheta = 174.4°$ and the dashed line using $m = 1$.

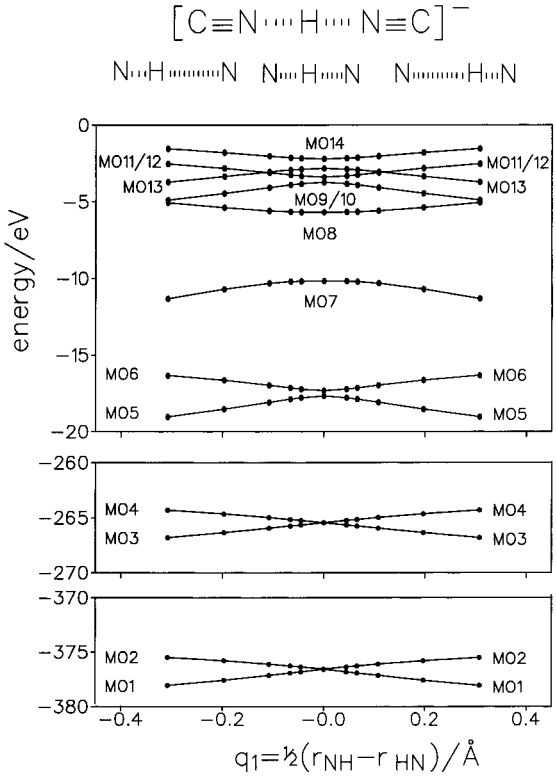

Figure 9. Energies of the 14 occupied molecular orbitals of [C≡N···H···N≡C]$^-$ (**1**) calculated using the deMon code as a function of the proton-transfer coordinate q_1.

present how the different molecular orbitals of **1** contribute to the couplings across the hydrogen bonds, as a function of the hydrogen bond geometry. In Figure 9 we have plotted the energies of the different molecular orbitals calculated using the deMon code, and in Figure 10 the orbitals are graphically represented. A detailed list of all coefficients is available in the Standard Supporting Information. There are 14 occupied orbitals. The four lowest ones in energy, MO1−MO4 refer to the core 1s orbitals of carbon and nitrogen. MO5−MO8 and MO13 and MO14 correspond to σ orbitals, whereas MO9−MO11 correspond to π orbitals. Finally, we have plotted in Figure 11 the contributions of the important MOs to the J_{NH} and J_{NN}.

First, we note that the core orbitals and the π orbitals do not contribute to both couplings. Moreover, the contribution of MO14 is very small and can be neglected. Second, the individual contributions of MO5 and MO6 are large but cancel each other to a large extent. In a similar way, the contributions of MO8 and MO13 also cancel each other partially. Therefore, the couplings J_{NH} and J_{NN} are almost exclusively defined by the contribution of MO7, and the sum of the contributions of MO5 + MO6 and of MO8 + MO13. In the case of J_{NH} the two latter terms are negative, but otherwise of a similar form as the contribution of MO7. By contrast, in the case of J_{NN}, MO7 plays a dominant role in the symmetric complex, whereas in the asymmetric complexes the sum of MO7 and MO8 dominates.

At present, it is difficult to derive a simple picture for the influence of the various MOs on the coupling constants. However, one striking fact is evident: MO7, MO8, and MO13 are the orbitals which exhibit non-negligible coefficients of atoms from both sides of the hydrogen bond, even in the asymmetric case. All other MOs become more localized when the proton is shifted to a given nitrogen atom.

The form of MO7 is especially striking. It is formed by a positive overlap of sp orbitals, one of each nitrogen, and of the s orbital of hydrogen. It does not exhibit a node in the region

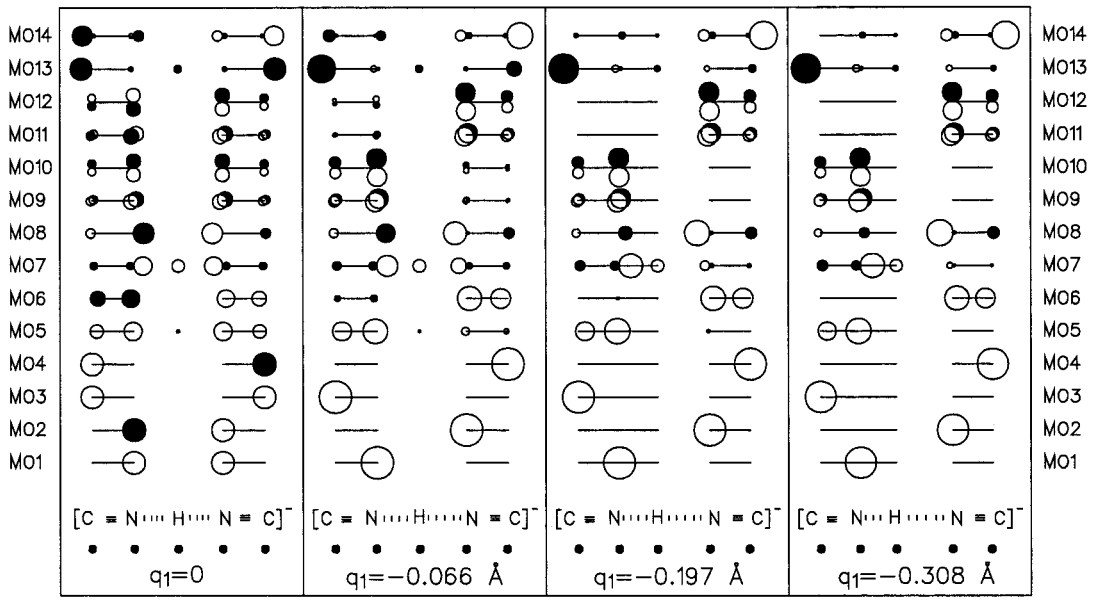

Figure 10. Graphical representation of the 14 occupied molecular orbitals of [C≡N···H···N≡C]$^-$ (**1**) calculated using the deMon code as a function of the proton-transfer coordinate q_1.

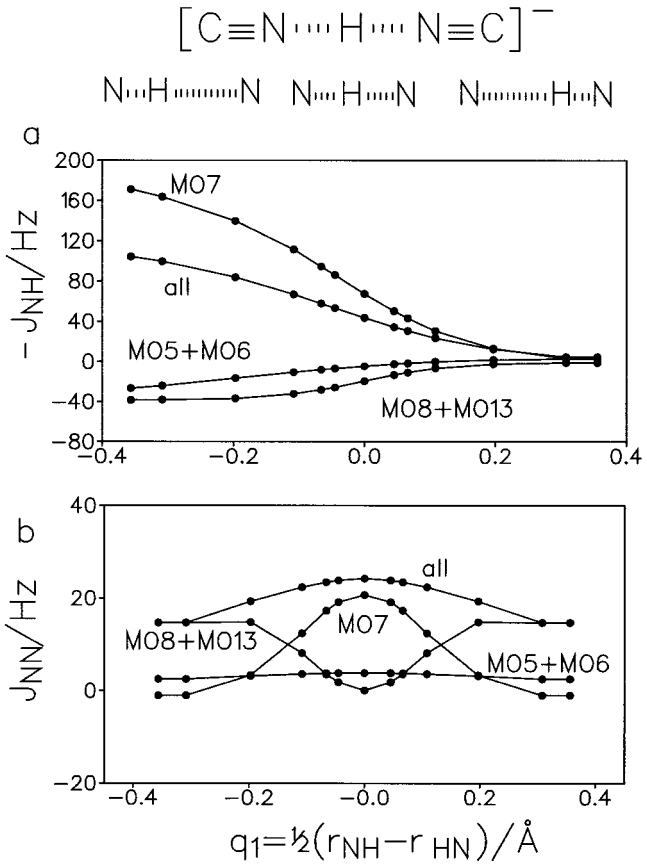

Figure 11. Individual contributions of molecular orbitals of [C≡N···H···N≡C]$^-$ (**1**) to the coupling constants J_{NH} and J_{NN} calculated using the deMon code as a function of the proton-transfer coordinate q_1.

of the hydrogen bond, even if the proton is shifted toward one of the nitrogen atoms. This only decreases the coefficient of the sp orbital of the more distant nitrogen. These findings are consistent with a covalent character of both the shorter and the longer N···H bond. As a consequence, the contribution of MO7 to J_{NH} follows in a monotonic way the NH-bond order, that is, becomes zero but not negative if the N···H distance increases. The second negative term in eq 8, therefore, might arise from the combined contribution of MO5, MO6, MO8, and MO13. Depending on the relative contributions J_{NH} is then negative, close to zero, or slightly positive, where the negative contribution dominated in the FHF case. In the NHN case the accuracy of the deMon code does not allow us to definitively state the sign of J_{NH} in the region where the values are of 1−2 Hz. The contribution of MO7 to J_{NN} is understandable in view of the almost direct spatial overlap of the two sp nitrogen orbitals. Naturally, this overlap is stronger in the symmetric complex when the distance of the two nitrogen atoms exhibits a minimum.

Conclusions

We have shown that the empirical valence bond model of the hydrogen bond can be used in order to derive useful equations which are able to relate calculated or experimental scalar coupling constants of hydrogen bond to the geometry of hydrogen bonds. This model works because of the well-known correlation between the two distances A···H and H···B of a hydrogen-bonded system A−H···B established previously by neutron diffraction studies,[2−4] NMR and theoretical calculations.[5] We showed that the deMon-NMR code[11] for the calculation of coupling constants is able to reproduce the experimental coupling constants in ^{15}N−H···^{15}N hydrogen-bonded systems, whereas in the case of ^{19}F−H···^{19}F hydrogen bonds only the general trend is verified. A very important result is that the coupling constant J_{AB} between the two heavy atom nuclei in a hydrogen bond A−H···B can be larger than J_{AH} or J_{HB}. It arises mainly from a direct positive overlap of the atomic orbitals of A and B and of H. A molecular orbital analysis showed that the appearance of coupling constants across the hydrogen bond is related to common molecular orbitals extending over both the proton donor and the acceptor. When the proton is shifted from A toward B, J_{AB} increases and exhibits a maximum at the shortest possible A···B distance in the symmetric or quasi-symmetric complex. The maximum coupling constant is slightly dependent on the hydrogen bond angle and on the type of the heavy atoms, but fairly independent of the chemical nature of the residues, in contrast to the coupling J_{AH}. This quantity decreases when the A···H distance is increased,

but can become negative and vanish only at large A···H distances. This effect arises from negative contributions of certain molecular orbitals. As a conclusion, vanishing scalar couplings J_H···B alone are no longer an indication of the noncovalent character of the hydrogen bond, whereas the value of the J_{AB} coupling give a crucial criterion.

Acknowledgment. We thank the Deutsche Forschungsgemeinschaft, Bonn-Bad Godesberg, the Fonds der Chemischen Industrie, Frankfurt, the Russian Foundation for Basic Research, grants 99-03-33163 and 97-03-33658a, for financial support. In Slovakia this work was supported by the Slovak Grant Agency VEGA (Project No. 1-4012/99). Computational resources of the Computing Center of the Slovak Academy of Sciences are acknowledged.

Note Added in Proof. During the revision of this manuscript a paper appeared,[20] reporting novel experimental and calculated coupling constants across NHN-hydrogen bonds of Watson−Crick nucleic acid base pairs including correlations between the coupling constants, proton chemical shifts, and hydrogen bond geometries. Most correlations were found to be quasi-linear within the limited range of hydrogen bond geometry variations of nucleic acid base pairs. Furthermore, Perera et al.[21] report a value of $J_{FF} = 225$ Hz for FHF^- calculated using improved ab initio methods. This value is in close agreement with the extrapolated experimental value reported in ref 8 and in this study.

Supporting Information Available: A detailed list of all molecular orbitals and energies of **1** at different hydrogen bond geometries as well as the contributions of the molecular orbitals to the coupling constants (PDF). This material is available free of charge via the Internet at http://pubs.acs.org.

JA9907461

(20) Dingley, A. J.; Masse, J. E.; Peterson, R. D.; Barfield, M.; Feigon, J.; Grzesiek, S. *J. Am. Chem. Soc.* **1999**, *121*, 6019.
(21) Perera, S. A.; Bartlett, R. J. *J. Am. Chem. Soc.* **2000**, *122*, 1231.